

# Simultaneous analysis of phytohormones, phytotoxins, and volatile organic compounds in plants

Eric A. Schmelz<sup>\*,†</sup>, Juergen Engelberth<sup>\*</sup>, Hans T. Alborn<sup>\*</sup>, Phillip O'Donnell<sup>‡</sup>, Matt Sammons<sup>\*</sup>, Hiroaki Toshima<sup>§</sup>, and James H. Tumlinson III<sup>\*</sup>

<sup>\*</sup>Center of Medical, Agricultural, and Veterinary Entomology, U. S. Department of Agriculture–Agricultural Research Service, 1600/1700 Southwest 23rd Drive, Gainesville, FL 32608; <sup>‡</sup>Department of Horticultural Sciences, University of Florida, Gainesville, FL 32611; and <sup>§</sup>Department of Bioresource Science, Ibaraki University, Ibaraki, Osaka 300-0393, Japan

Contributed by James H. Tumlinson III, June 12, 2003

Phytohormones regulate the protective responses of plants against both biotic and abiotic stresses by means of synergistic or antagonistic actions referred to as signaling crosstalk. A bottleneck in crosstalk research is the quantification of numerous interacting phytohormones and regulators. The chemical analysis of salicylic acid, jasmonic acid, indole-3-acetic acid, and abscisic acid is typically achieved by using separate and complex methodologies. Moreover, pathogen-produced phytohormone mimics, such as the phytotoxin coronatine (COR), have not been directly quantified in plant tissues. We address these problems by using a simple preparation and a GC-MS-based metabolic profiling approach. Plant tissue is extracted in aqueous 1-propanol and mixed with dichloromethane. Carboxylic acids present in the organic layer are methylated by using trimethylsilyldiazomethane; analytes are volatilized under heat, collected on a polymeric absorbent, and eluted with solvent into a sample vial. Analytes are separated by using gas chromatography and quantified by using chemical-ionization mass spectrometry that produces predominantly  $[M+H]^+$  parent ions. We use this technique to examine levels of COR, phytohormones, and volatile organic compounds in model systems, including *Arabidopsis thaliana* during infection with *Pseudomonas syringae* pv. *tomato* DC3000, corn (*Zea mays*) under herbivory by corn earworm (*Helicoverpa zea*), tobacco (*Nicotiana tabacum*) after mechanical damage, and tomato (*Lycopersicon esculentum*) during drought stress. Numerous complex changes induced by pathogen infection, including the accumulation of COR, salicylic acid, jasmonic acid, indole-3-acetic acid, and abscisic acid illustrate the potential and simplicity of this approach in quantifying signaling crosstalk interactions that occur at the level of synthesis and accumulation.

Phytohormones regulate numerous aspects of plant growth, development, and response to stress. Historically, phytohormone signals were examined as individual pathways mediating a given response to a stimulus. Phytohormones are now recognized as functioning in complex signaling networks, often with interactive effects, referred to as crosstalk, on the expression of plant responses to stresses such as drought, wounding, or insect and pathogen attack (1–3). Positive and negative interactions on the expression of chemical and molecular responses have been described for jasmonic acid (JA)–ethylene (E) (4–6), salicylic acid (SA)–E (7–9), and SA–JA (10–12). It is now established that the coordinated interactions of JA, SA, and E control plant responses after biotic stress (13). Likewise, complex sequences of phytohormone interactions have been described after pharmacological treatments and pathogen infection (14, 15). Recent work demonstrating networks of phytohormone signaling interactions brings increased interest in the development and use of multicomponent phytohormone analyses for elucidating these interactions.

Alterations in the synthesis or perception of one signal can influence the dynamics of nontarget signals. For example, tomato plants deficient in either E production or perception failed to exhibit typical patterns of chlorosis and necrosis after infection with *Xanthomonas campestris* pv. *vesicatoria* (9). Pathogen-

induced SA accumulation, responsible for the typical expanded cell-death responses, was found to be E dependent (9). During infection with *Xanthomonas campestris* pv. *campestris*, *Arabidopsis* also displays cooperative E and SA action in disease symptom development; the order of events, however, is opposite from that of tomato (10). In a search for signal-transduction mutants insensitive to exogenous cytokinins, candidate genes were found to be allelic to *EIN2*, a gene in the E-response pathway (16). Cytokinin application stimulates E production by increasing the stability of 1-aminocyclopropane-1-carboxylate synthase proteins (17). Sugar signaling can also act at the level of phytohormone biosynthesis. Recent cloning of *GLUCOSE INSENSITIVE1* revealed that the abscisic acid (ABA) biosynthetic pathway is linked to glucose sensing (18).

Phytohormone interactions are commonly considered at the level of signal transduction without proper consideration of phytohormone synthesis or accumulation (19). Many regulators influence the levels of additional phytohormones; thus, crosstalk interactions can occur at the level of production. The elucidation of pleiotropic and often unpredicted effects has been hampered by the inaccessibility of multiple phytohormone analyses. Numerous methods exist for the direct chemical quantification of individual phytohormones, regulators, and also volatile organic compounds (VOCs) that can function as ecological signals (20–26). These techniques are often characterized by time-consuming protocols, multiple purification steps, and few target analytes. An objective of GC-MS-based analysis of chemical signals is the inclusive metabolic profiling of key analytes (27–29). Toward this goal, we describe a simple method with broad potential applicability in the preparation and simultaneous GC-MS analysis of the pathogen-derived phytotoxin coronatine (COR), multiple phytohormones [SA, JA, indole-3-acetic acid (IAA), and ABA], and VOCs from milligram amounts of plant tissue. This readily available technology enables the exploration of interactions between physiologically and ecologically relevant chemical signals at the level of production; it also makes it possible to readdress previous findings in a comprehensive manner.

## Materials and Methods

**Plant, Insect, and Pathogen Material.** Growth conditions of corn (*Zea mays* cv. Delprim), tobacco (*Nicotiana tabacum* cv. Samsun-NN), tomato (*Lycopersicon esculentum* cv. Luckulus), and *Arabidopsis thaliana* cv. Columbia (Col-0) have been reported (7, 8, 29, 30). Early third-instar corn earworm (CEW) larvae (*Helicoverpa zea*) were reared on corn meal and molasses.

Abbreviations: ABA, abscisic acid; BA, benzoic acid; CA, *trans*-cinnamic acid; CEW, corn earworm; COR, coronatine; dhJA, dihydro-JA; E, ethylene; FW, fresh weight; I-Ile, *N*-indanolyl-L-isoleucine; IAA, indole-3-acetic acid; JA, jasmonic acid; JA-Leu, *N*-jasmonoyl-L-leucine; ME, methyl ester; *Pst*, *Pseudomonas syringae* pv. *tomato* DC3000; SA, salicylic acid; VOCs, volatile organic compounds; VPE, vapor-phase extraction.

See commentary on page 10144.

<sup>†</sup>To whom correspondence should be addressed. E-mail: eschmelz@gainesville.usda.uffl.edu.

*coverpa zea*), used in the herbivory trial, were obtained from W. J. Lewis (U.S. Department of Agriculture–Agricultural Research Service, Tifton, GA). Culture of *Pseudomonas syringae* pv. *tomato* DC3000 (*Pst*) and infection of *Arabidopsis* plants have been described (8).

**Chemicals.** Indole,  $\beta$ -caryophyllene,  $\alpha$ -humulene, benzoic acid (BA), BA methyl ester (ME), SA, SA-ME, *trans*-cinnamic acid (CA), CA-ME, JA, JA-ME, IAA, IAA-ME, and ABA were purchased from either Aldrich or Sigma. Dihydro-JA (dhJA)-ME (Bedoukian Research, Danbury, CT) was subjected to alkaline hydrolysis to yield dhJA. *N*-jasmonoyl-L-leucine (JA-Leu), *N*-indanoyl-L-isoleucine (I-Ile), and COR were synthesized and purified by using established methods (31–33). Isotopically labeled internal standards, including [ $^2\text{H}_5$ ]IAA, [ $^2\text{H}_6$ ]SA, and [ $^2\text{H}_5$ ]CA were purchased from CDN Isotopes (Pointe-Claire, QC, Canada); [ $^{13}\text{C}_6$ ]BA and [ $^2\text{H}_6$ ]ABA were purchased from ICON Isotopes (Summit, NJ).

**Sample Preparation.** Plant tissues were frozen and ground in liquid  $\text{N}_2$ ; 200 mg of each sample was transferred to 2-ml screw-cap FastPrep tubes (Qbiogene, Carlsbad, CA) containing 1 g of Zirmil beads (1.1 mm; SEPR Ceramic Beads and Powders, Mountainside, NJ). dhJA and isotopically labeled internal standards (100 ng each in 5  $\mu\text{l}$  of EtOH) were added to the 2-ml tubes before sample addition. The samples were mixed with 300  $\mu\text{l}$  of 1-propanol/ $\text{H}_2\text{O}$ /concentrated HCl (2:1:0.002, vol/vol) and shaken for 30 s in a FastPrep FP 120 tissue homogenizer (Qbiogene). Methylene chloride (1 ml) was added to each sample, followed by reshaking for 5 s in the homogenizer, and centrifugation at  $11,300 \times g$  for 30 s. The bottom methylene chloride/1-propanol layer was then transferred to a 4-ml glass screw-cap vial. Carboxylic acids were converted into MEs by the addition of 2  $\mu\text{l}$  of 2.0 M trimethylsilyldiazomethane in hexane (Aldrich). The vials were then capped and allowed to sit at room temperature for 30 min. Excess trimethylsilyldiazomethane was then destroyed by adding 2  $\mu\text{l}$  of 2.0 M acetic acid in hexane to each sample.

Volatile metabolites were separated from the complex mixture by a process we termed vapor-phase extraction (VPE). Teflon-lined caps were replaced with open-top caps fitted with Thermogreen septa (11 mm; Supelco). An inert filter trap (29), containing  $\approx 20$  mg of SuperQ (Alltech Associates), was inserted through septum along with a 22-gauge needle carrying a low-pressure  $\text{N}_2$  stream. A  $\text{N}_2$  flow rate of  $500 \text{ ml} \cdot \text{min}^{-1}$  through the trap was created with a Tygon vacuum line and diaphragm vacuum pump (KNF Neuberger, Trenton, NJ) calibrated with a needle valve and flow meter. The vials were placed into an aluminum heating block at  $70^\circ\text{C}$  until all solvent vaporized and moved through the system. The dry vial was then transferred to a second heating block at  $200^\circ\text{C}$  for 2 min. These elevated temperatures were required to aid in the recovery of less volatile compounds. The trapped volatiles were then eluted with 150  $\mu\text{l}$  of methylene chloride and analyzed by GC-MS. SuperQ traps were unharmed and rinsed with 200  $\mu\text{l}$  of methylene chloride immediately before each reuse.

**Quantification and Recovery.** GC-MS conditions and quantification were described (29). The method used a quadropole MS system (5890GC connected to a 5973 Mass Selective Detector; Agilent, Palo Alto, CA) with isobutane chemical ionization and selected-ion monitoring (selected ion  $\pm 0.7$  mass unit). Twelve test compounds, consisting of VOCs and carboxylic acid MEs were measured by using selected-ion monitoring with retention times and  $[\text{M}+\text{H}]^+$   $m/z$  ions as follows (numbering corresponds to that in Figs. 1 and 2): 1, BA-ME (7.55 min, 137); 2, SA-ME (8.62 min, 153); 3, indole (9.46 min, 118); 4, CA-ME (10.35 min, 163); 5,  $\beta$ -caryophyllene (11.02 min, 205); 6,  $\alpha$ -humulene (11.29

min, 205); 7, JA-ME (*trans* 12.48 min, *cis* 12.71 min, 225); 8, IAA-ME (13.62 min, 190); 9, ABA-ME (15.53 min, 279); 10, JA-Leu-ME (17.96 min, 338); 11, I-Ile-ME (18.76 min, 304); and 12, COR-ME (19.80 min, 334). Internal standards with the corresponding retention times and  $[\text{M}+\text{H}]^+$   $m/z$  ions were as follows: [ $^{13}\text{C}_6$ ]BA-ME (7.55 min, 143), [ $^2\text{H}_6$ ]SA-ME (8.61 min, 157), [ $^2\text{H}_5$ ]CA-ME (10.33 min, 168), dhJA-ME (*trans* 12.53 min, *cis* 12.75 min, 227), [ $^2\text{H}_5$ ]IAA-ME (13.61 min, 195), and [ $^2\text{H}_6$ ]ABA-ME (15.50 min, 285). The [ $^2\text{H}_6$ ]SA internal standard was converted to [ $^2\text{H}_4$ ]SA-ME during sample processing to give a 157  $[\text{M}+\text{H}]^+$  ion instead of 159. The 279 and 285 parent  $[\text{M}+\text{H}]^+$  ions for ABA-ME and [ $^2\text{H}_6$ ]ABA-ME fragment to produce predominantly 261 and 267  $[\text{M} - \text{H}_2\text{O} + 1]^+$  ions, respectively. Thus, these ions were used routinely for ABA-ME quantification purposes.

Recovery of the 12 unlabeled test compounds was first calculated based on the peak area of the selected ions and the slope of an external standard curve constructed from pure synthetic VOCs and carboxylic acid MEs. Untreated corn leaf tissue (200 mg) was spiked with 0, 10, 25, 50, 100, and 150 ng each of the three VOCs and nine free acids ( $n = 4$ ) and prepared by using the protocol above. By using [ $^{13}\text{C}_6$ ]BA, [ $^2\text{H}_6$ ]SA, [ $^2\text{H}_5$ ]CA, dhJA, [ $^2\text{H}_5$ ]IAA, and [ $^2\text{H}_6$ ]ABA as internal standards, we performed a second recovery estimate on BA, SA, CA, JA, IAA, and ABA. Corn tissue samples were spiked with 0, 10, 25, 50, 75, and 100 ng of each of these six unlabeled free acids ( $n = 4$ ) and 100 ng each of the corresponding internal standards as free acids.

**Analyte Confirmation.** Structural confirmation was performed on selected samples and authentic standards by using GC-MS/MS with methanol chemical ionization (Trace GC 2000 connected to a GCQ mass spectrometer, Thermo Finnigan, San Jose, CA). The GC and MS conditions as described (28, 29) with the following modifications. All components of interest were analyzed by using a scan time of 0.53 s with three micro scans and a maximum ionization time of 25 ms. Parent-ion selection was switched segmentally within each run with an isolation window of  $\pm 2$  mass units for each parent ion and with an isolation time of 8 ms. The ion source temperature, collision energy, main radio-frequency voltage, and collision time were  $200^\circ\text{C}$ , 2.0 V, 0.450 V, and 30 ms, respectively.

**Biotic and Abiotic Stress Experiments.** *Arabidopsis*, corn, tobacco, and tomato were used to examine plant responses to *Pst* infection, insect herbivory, wounding, and drought, respectively. In all experiments plant tissues were harvested, frozen in liquid  $\text{N}_2$ , pulverized, and stored at  $-80^\circ\text{C}$  before analysis. Six-week-old *Arabidopsis* plants were either mock-inoculated ( $n = 3$ ) or infected with *Pst* ( $n = 3$ ) and successively harvested at 0, 12, 24, and 48 h after treatments as described (8). Insect infestation of 12-day-old corn seedlings was achieved by placing five third-instar CEW caterpillars on plants at 6 p.m. as described (30). Infested ( $n = 5$ ) and uninfested ( $n = 5$ ) plants were harvested 18 h later in the middle of the light cycle. On average, this level of CEW herbivory resulted in a 20% loss in leaf area. Leaf-wound treatments were performed by using a fabric-pattern wheel on 5-week-old tobacco plants in the middle of the light cycle as described in previous time-course experiments (34). After 6 h, leaves 2–5 were harvested from both wounded and unwounded control plants ( $n = 4$ ). Drought was induced in 6-week-old tomato plants, containing five fully expanded leaves, by withholding water and allowing the soil to dry partially for 48 h. At this time, leaves 3 and 4 were harvested from stressed ( $n = 4$ ) and well watered plants ( $n = 4$ ).

## Results and Discussion

**Recovery and Analysis of Analytes.** The method resulted in a high level of recovery, reproducibility, and linearity in the quantifi-

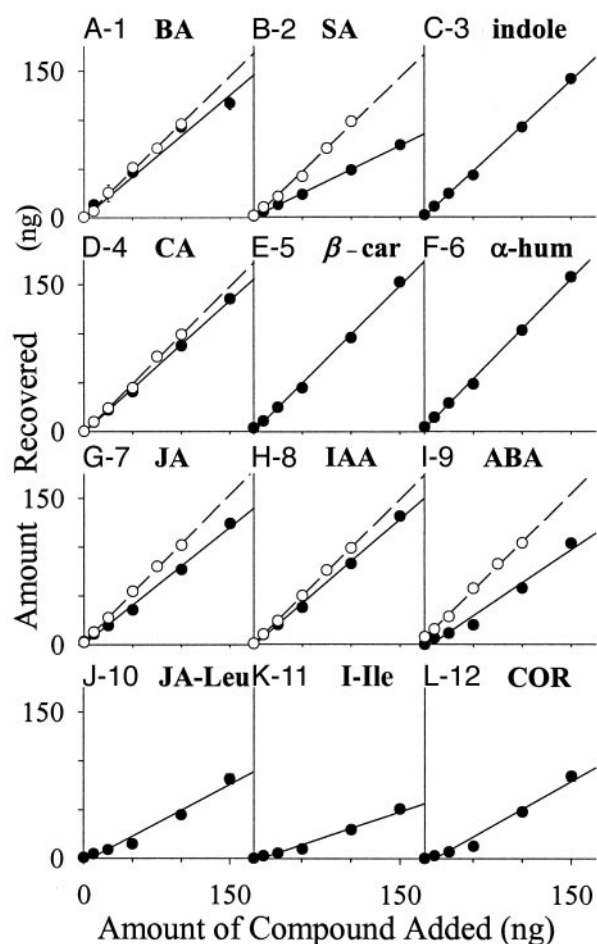


**Fig. 1.** Recovery and quantification of 12 synthetic analytes with VPE by using internal and external standards. Total recovery (●) was calculated by adding 0, 10, 25, 50, 100, or 150 ng of the following VOCs and free carboxylic acids to plant tissue samples (200 mg). (A-1) BA ( $y = 0.84x$ ). (B-2) SA ( $y = 0.50x$ ). (C-3) Indole ( $y = 0.93x$ ). (D-4) CA ( $y = 0.90x$ ). (E-5)  $\beta$ -Caryophyllene ( $\beta$ -car;  $y = 0.99x$ ). (F-6)  $\alpha$ -Humulene ( $\alpha$ -hum;  $y = 1.01x$ ). (G-7) JA ( $y = 0.80x$ ). (H-8) IAA ( $y = 0.86x$ ). (I-9) ABA ( $y = 0.68x$ ). (J-10) JA-Leu ( $y = 0.53x$ ). (K-11) I-Ile ( $y = 0.34x$ ). (L-12) COR ( $y = 0.57x$ ). Sample preparation followed the described VPE protocol (see *Materials and Methods*), and  $[M+H]^+$   $m/z$  MS responses were compared with the slope of external standard curves generated for each VOC and carboxylic acid ME. By using commercially available internal standards for BA (A-1,  $y = 0.96x$ ), SA (B-2,  $y = 0.96x$ ), CA (D-4,  $y = 0.99x$ ), JA (G-7,  $y = 1.00x$ ), IAA (H-8,  $y = 0.99x$ ), and ABA (I-9,  $y = 0.99x$ ), a second estimate for recovery (○) was made that computationally corrected for losses. Slopes ( $y$ ), correlation coefficients (all  $r^2 \geq 0.97$ ), and error bars (mean  $\pm$  SEM,  $n = 4$ , obscured by plot symbols) indicate the recoveries, accuracy, and reproducibility of this method for each analyte.

cation of 12 test compounds (Fig. 1). All naturally occurring analytes were recovered from plant extracts with 50% or greater efficiency. The lowest recovery found (30%) was for the synthetic elicitor I-Ile (Fig. 1K). Recovery of free acids spiked into plant extracts was based on the slope of selected-ion monitoring external standard curves of carboxylic acid MEs and, thus, is a conservative estimate. As expected, recovery was reduced for the higher mass analytes with lower volatility, such as ABA-ME and COR-ME (Fig. 1 I–L). Recoveries for VOCs such as indole,  $\beta$ -caryophyllene, and  $\alpha$ -humulene are near 100% (Fig. 1 C, E, and F). Use of isotopic and saturated internal standards computationally corrected for the imperfect recovery of BA, SA, CA, JA, IAA, and ABA (Fig. 1 A, B, D, and G–I). Importantly, the VPE technique displayed a high degree of reproducibility and linearity with all correlation coefficients ( $r^2$ )  $>0.97$  (Fig. 1).

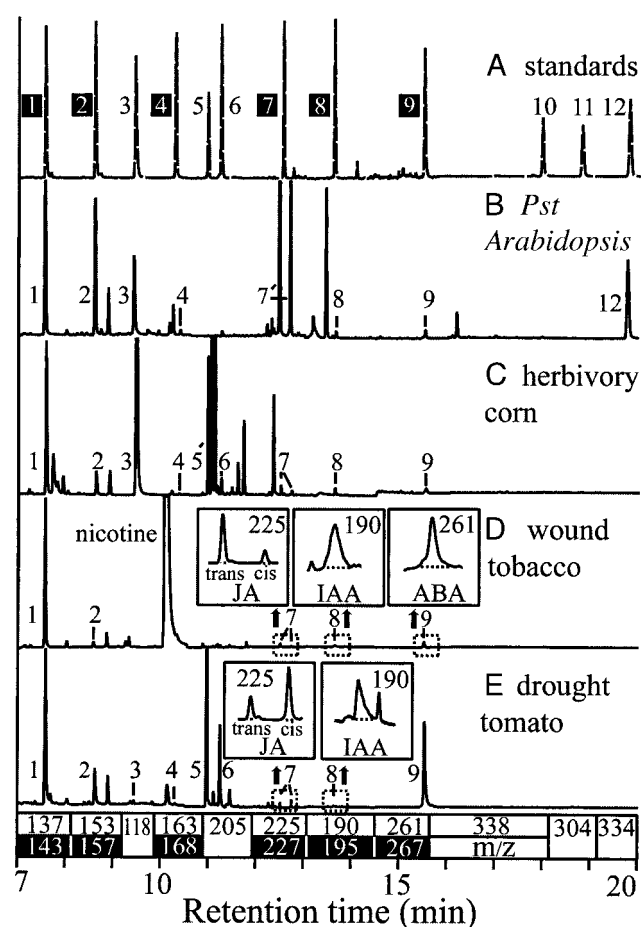


**Fig. 2.** (A) In a plant matrix background, selected-ion chromatograms of the internal and external standards for the VOCs and carboxylic acid MEs (white numbers on black background indicate isotopically labeled compounds): 1,  $[^{13}C_6]$ BA-ME; 2,  $[^2H_4]$ SA-ME; 3, indole; 4,  $[^2H_5]$ CA-ME; 5,  $\beta$ -caryophyllene; 6,  $\alpha$ -humulene; 7, dhJA-ME; 8,  $[^2H_5]$ IAA-ME; 9,  $[^2H_6]$ ABA-ME; 10, JA-Leu-ME; 11, I-Ile-ME; and 12, COR-ME. (B–E) Proportionally scaled single-ion chromatograms of endogenous analytes for *Pst*-infected *Arabidopsis* (B), CEW herbivory on corn (C), wounded tobacco (D), and drought-stressed tomato (E). Endogenous compounds confirmed and quantified include: 1, BA-ME; 2, SA-ME; 3, indole; 4, CA-ME; 5, caryophyllene; 7, JA-ME; 8, IAA-ME; 9, ABA-ME; and 12, COR-ME. Because of the presence of secondary metabolites, phytohormones appear visually as minor components; examples of expanded single-ion chromatograms for JA, IAA, and ABA are illustrated in tobacco and tomato (Insets in D and E). The x axis denotes GC retention times and  $[M+H]^+$   $m/z$  ions used for quantitation purposes of internal standards (black background) and native analytes (white background). The y axis is the relative ion intensity (%).

A composite selected-ion chromatogram of the internal and external standards is displayed in Fig. 2A. Representative samples of *Pst*-infected *Arabidopsis*, herbivore-attacked corn, wounded tobacco, and drought-stressed tomato are illustrated in separate traces (Fig. 2B–E). In this comparison, high levels of stress-induced analytes were detected in the following: JA/COR in *Arabidopsis* (Fig. 2B), indole and  $\beta$ -caryophyllene in corn (Fig. 2C), and ABA in tomato (Fig. 2E). In general, levels of CA and JA-Leu detected were extremely low, displayed no clear patterns, and consequently were not summarized. I-Ile and  $\alpha$ -humulene were included only for method-development purposes. Features of this method are illustrated in Fig. 2B–E. Methylated phytohormones are typically minor components in the GC-MS ion chromatogram trace, and occasionally other plant constituents may interfere with the quantification of a component. In tobacco, for example, nicotine has the same  $[M+H]^+$  ion ( $m/z$



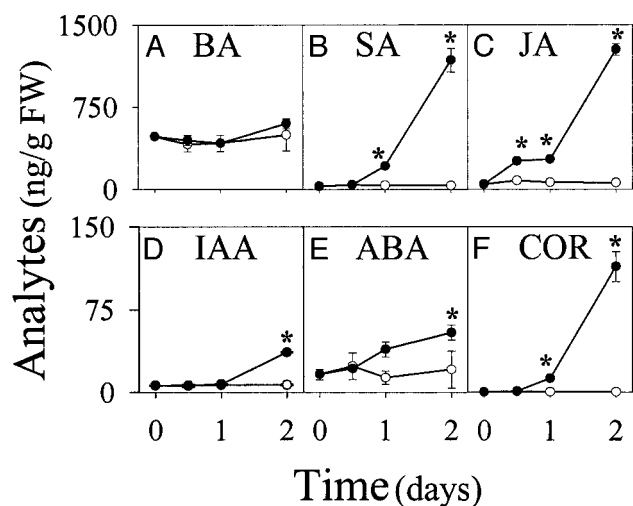


**Fig. 3.** Infection of *Arabidopsis* with *Pst* results in large-scale profile changes over time. Shown are mean ( $\pm$ SEM,  $n = 3$ ) BA, SA, JA, IAA, ABA, and COR (A–F, respectively) tissue levels (ng/g FW) of control (○) and *Pst*-infected (●) leaf tissue. Asterisks denote significant increases above the time 0 control ( $P < 0.05$ , Dunnett's test).

163) and elutes near CA-ME (Fig. 2D). Thus, the identity of individual peaks needs to be confirmed within each plant species examined. Importantly, with proper chromatographic separation, this complexity is a significant advantage. In preliminary studies, we now detect a wide range of fatty acids, including linolenic acid and 12-oxophytodienoic acid by using this method; thus, Fig. 2 displays only a fraction of the available information useful in GC-MS-based metabolic-profiling studies.

***Pst* Infection Results in COR Accumulation and Widespread Changes.** Phytohormone signaling during *Pseudomonas* infection is complex with interactions of E, SA, and JA currently under investigation (3, 35). Pathogen-produced phytotoxins, such as COR, are believed to regulate the level of infection (36, 37), function as signal mimics (38), and induce the production of E (39). Despite the role of COR in disease progression and as a mediator of crosstalk interactions, chemical analysis of COR within infected plant tissues has not been previously reported. COR quantification has been limited to bacterial culture broth (24, 36), enzyme-linked immunosorbent assays for localization studies (40), and bioassays based on hypertrophic reactions in potatoes (41). In *Arabidopsis* leaf tissue, we demonstrate significant increases in COR levels within 24 h of *Pst* infection and average levels of 110 ng/g of fresh weight (FW) after 48 h (Fig. 3F). This pattern is mirrored by increases in SA levels (Fig. 3B).

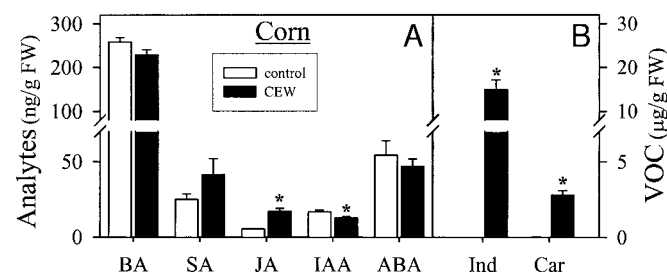


**Fig. 4.** CEW herbivory induces levels of JA and volatile metabolites but reduces IAA. (A) Mean ( $\pm$ SEM,  $n = 5$ ) BA, SA, JA, IAA, and ABA levels (ng/g FW) of corn plants 18 h after initiation of herbivory. (B) Mean levels of the VOCs ( $\mu$ g/g FW), indole (Ind) and caryophyllene (Car), induced by CEW herbivory. Asterisks denote significant differences between treatments ( $P < 0.05$ ,  $t$  test).

Both free SA levels and COR are associated with chlorotic lesions (8, 42); likewise, both COR perception and SA accumulation are required for symptom development (43). COR is structurally similar to 12-oxophytodienoic acid, a mimic of jasmonate signals (38), and displays 100–10,000 times greater activity than JA in selected bioassays (44, 45). In *Arabidopsis*, COR stimulates increased JA levels first at 24 h, followed by large increases after 48 h (46). In the present study, *Pst*-induced increases in JA were rapid (12 h) and preceded increases in COR; COR accumulation, however, may drive the subsequent increases in JA levels (Fig. 3C). Given the activity of COR and its influence on multiple phytohormones, knowledge of tissue levels will aid in clarifying signaling crosstalk interactions that may occur during *Pst* infection.

*Pst* infection also induces increases in IAA and ABA levels (Fig. 3D and E). The function of pathogen-induced increases in IAA levels remains to be clarified because this phenomenon has been described only recently in *Arabidopsis* after *Xanthomonas campestris* infection (8). The biosynthetic source of the induced IAA levels is also unclear because multiple plant pathogenic bacteria harbor the *iaaM* and *iaaH* genes that convert tryptophan to IAA through an indole-3-acetamide intermediate (47). The induction of IAA levels in *Xanthomonas campestris* pv. *vesicatoria*-infected *Arabidopsis* was judged to be plant derived based on the absence of such genes in the reported genome (8). Similarly, the induction of ABA levels by fungal pathogens has been reported in tomato with a portion of the ABA being pathogen derived (48). In *Pst*-infected *Arabidopsis*, induced increases in ABA are small and likely a secondary response to biotic stress.

**Herbivory Increases JA, Decreases IAA, and Stimulates Production of VOCs.** Increases in both E and JA after caterpillar herbivory have been reported widely (6, 30, 49); in contrast, insect-induced SA levels come from a single study of cotton (50) and a long-term infestation of excised lima bean leaves with herbivorous spider mites (51). Thus, with the exception of JA and E, general patterns of phytohormone responses to insect herbivory are unclear. CEW herbivory on corn seedlings resulted in a significant 3.1-fold increase in JA levels and a 1.3-fold decrease in IAA levels (Fig. 4A). In tobacco, reduced IAA levels after wounding (52) have been described and may play a role as exogenous IAA inhibits wound-induced JA levels (34) and protease inhibitor gene expression (52). Antagonism between JA and IAA signaling has been suggested during wounding (52) but not previously considered in the context of herbivory. No significant changes in BA, SA, or ABA levels were detected after 24 h of CEW herbivory (all  $F_{1,8}$  values  $< 3.57$ ,  $P$  values  $> 0.09$ ). Consistent with this result, *Arabidopsis* plants expressed lower levels of water-stress-induced genes when attacked by *Pieris rapae* caterpillars compared with mechanical wounding alone (53).

In corn, caterpillar-induced JA triggers VOC emissions (26, 30, 54, 55) that can function as indirect plant defenses by means of the attraction of natural enemies (56, 57). This process is now recognized as regulating important multitrophic interactions in both agricultural and natural systems (58, 59). Tissue levels of  $\beta$ -caryophyllene and indole, used as markers for induced VOC emission, were increased 70- and 1,850-fold, respectively, by CEW herbivory (Fig. 4B). These induced tissue levels strongly suggest that herbivore-induced VOC emission in corn is the result of increased biosynthesis and release.

**Wounding Alters JA, IAA, and ABA Levels, Whereas Drought Induces Only ABA.** In tobacco, individual phytohormones investigated after wounding include homeostatic SA levels (60), decreased IAA levels (52), and increased ABA (61) and JA levels (34). By using 6 h as an intermediate time point, we confirm these diverse results in a single experiment (Fig. 5A). Consistent with previous

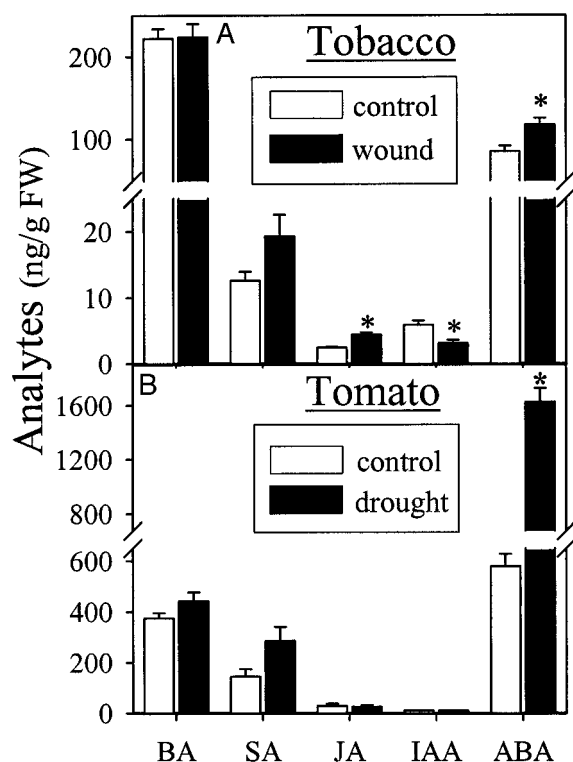


**Fig. 5.** Wounding increases JA and ABA but reduces IAA levels in tobacco, whereas drought stress selectively increases ABA levels in tomato. Mean ( $\pm$ SEM,  $n = 4$ ) BA, SA, JA, IAA, and ABA levels (ng/g FW) in tobacco leaves 6 h after treatment (A) and tomato leaves (B). Potted plants were drought stressed by withholding water with leaf tissue harvested after 48 h showing early visual symptoms of reduced turgor. Asterisks denote significant differences between treatments ( $P < 0.05$ ,  $t$  test).

reports, levels of SA and BA are not significantly altered after mechanical damage (all  $F_{1,6}$  values  $< 3.60$ ,  $P$  values  $> 0.10$ ) (60). Damage-induced accumulation of JA is rapid and transient, yet a significant 1.8-fold increase is still detected at 6 h (Fig. 5A). Wound-induced JA levels mediate increases in protease inhibitors and nicotine that, in turn, decrease the nutritive value of the tissues to herbivores (34, 62). In solanaceous plants, wound-induced increases in ABA and decreases in IAA are accentuated after 24 h (52, 63), yet these patterns were confirmed with a 1.4-fold increase in ABA and a 1.9-fold decrease in IAA within 6 h (Fig. 5A). In tobacco, reduced IAA levels after wounding have been described and suggest antagonism between JA and

IAA signals. These interactions, however, remain unclear (34, 52, 64).

In tomato, ABA is believed to have a primary role in mediating drought stress responses and a minor role in wound-defense signaling (65). Water deficiency imposed on tomato plants for 48 h resulted in water-stressed leaves that exhibited 2.8-fold increases in ABA levels (Fig. 5B). Similar drought-induced ABA responses have been described widely in plants (66). Interestingly, levels of BA, SA, JA, and IAA in water-stressed plants did not differ significantly from controls. Mean levels of SA in water-stressed leaves appeared 2-fold greater than controls; this trend, however, was not significant ( $F_{1,6} = 5.35$ ,  $P > 0.06$ ). ABA influences the regulation of plant water balance and is linked to reductions in stomatal aperture and induction of gene expression leading to the synthesis of osmoprotectants and damage-repair related proteins (67, 68).

**Concluding Remarks.** We present a facile, rapid, and inclusive analytical method that quantifies multiple phytohormones, COR, and VOCs simultaneously in small amounts of plant tissue. Changes in an array of physiological and ecological signals that accumulate in plant tissues during abiotic and biotic stress can now be accessed easily. The phytotoxin COR was also included in the chemical analysis of *Pst*-induced phytohormone changes. In *Arabidopsis*, we demonstrate that JA induction precedes the subsequent parallel increases in COR and SA. *Pst*-induced increases in IAA contrast with the suppression of IAA after herbivory and wounding. By illustrating snapshots of complex processes, namely multiple stresses in several plant species, we attempt to highlight the utility and potential of the VPE method in exploring phytohormone crosstalk interactions. Expansion of this technique to additional analytes is limited primarily by the acquisition of labeled and unlabeled standards for quantification and verification purposes. For example, JA is but one member of a large class of related biologically active oxylipins (53) that should be amenable to this method. The VPE technique utilizes readily available materials and produces a sample that is GC compatible and can be routinely analyzed at any facility with access to chemical-ionization–GC–MS. Genomic and microarray-based approaches are increasing our knowledge of phytohormone-mediated regulation exponentially at the mRNA level. Commensurate metabolic profiling approaches, such as this work and others (28), will enable the elucidation of networks of phytohormone interactions that regulate the developmental and defense responses to biotic and abiotic stress.

We thank reviewers for helpful advice that significantly improved the manuscript. This work was supported by funds from the U.S. Department of Agriculture–Agricultural Research Service and the Defense Advanced Research Project Agency.

1. Zhu, J. K. (2002) *Annu. Rev. Plant Biol.* **53**, 247–273.
2. de Bruxelles, G. L. & Roberts, M. R. (2001) *Crit. Rev. Plant Sci.* **20**, 487–521.
3. Kunkel, B. N. & Brooks, D. M. (2002) *Curr. Opin. Plant Biol.* **5**, 325–331.
4. Xu, Y., Chang, P. F. L., Liu, D., Narasimhan, M. L., Raghothama, K. G., Hasegawa, P. M. & Bressan, R. A. (1994) *Plant Cell* **6**, 1077–1085.
5. Zhu-Salzman, K., Salzman, R. A., Koiwa, H., Murdock, L. L., Bressan, R. A. & Hasegawa, P. M. (1998) *Physiol. Plant.* **104**, 365–372.
6. Kahl, J., Siemens, D. H., Aerts, R. J., Gabler, R., Kuhnemann, F., Preston, C. A. & Baldwin, I. T. (2000) *Planta* **210**, 336–342.
7. O'Donnell, P. J., Jones, J. B., Antoine, F. R., Ciardi, J. & Klee, H. J. (2001) *Plant J.* **25**, 315–323.
8. O'Donnell, P. J., Schmelz, E. A., Moussatche, P., Lund, S. T., Jones, J. B. & Klee, H. J. (2003) *Plant J.* **33**, 245–257.
9. Berrocal-Lobo, M., Molina, A. & Solano, R. (2002) *Plant J.* **29**, 23–32.
10. Doares, S. H., Narvaez-Vasquez, J., Conconi, A. & Ryan, C. A. (1995) *Plant Physiol.* **108**, 1741–1746.
11. O'Donnell, P. J., Calvert, C., Atzorn, R., Wasternack, C., Leyser, H. M. O. & Bowles, D. J. (1996) *Science* **274**, 1914–1917.

12. Rao, M. V., Lee, H., Creelman, R. A., Mullet, J. E. & Davis, K. R. (2000) *Plant Cell* **12**, 1633–1646.
13. Reymond, P. & Farmer, E. E. (1998) *Curr. Opin. Plant Biol.* **1**, 404–411.
14. Hansen, H. & Grossmann, K. (2000) *Plant Physiol.* **124**, 1437–1448.
15. Veselov, D., Langhans, M., Hartung, W., Aloni, R., Feussner, I., Götz, C., Veselova, S., Schlömski, S., Dickler, C., Bächmann, K., et al. (2003) *Planta* **216**, 512–522.
16. Cary, A. J., Liu, W. N. & Howell, S. H. (1995) *Plant Physiol.* **107**, 1075–1082.
17. Chae, H. S., Faure, F. & Kieber, J. J. (2003) *Plant Cell* **15**, 545–559.
18. Cheng, W. H., Endo, A., Zhou, L., Penney, J., Chen, H. C., Arroyo, A., Leon, P., Nambara, E., Asami, T., Seo, M., et al. (2002) *Plant Cell* **14**, 2723–2743.
19. Moller, S. G. & Chua, N. H. (1999) *J. Mol. Biol.* **293**, 219–234.
20. Uknes, S., Winter, A. M., Delaney, T., Vernooij, B., Morse, A., Friedrich, L., Nye, G., Potter, S., Ward, E. & Ryals, J. (1993) *Mol. Plant–Microbe Interact.* **6**, 692–698.
21. Mueller, M. J. & Brodschelm, W. (1994) *Anal. Biochem.* **218**, 425–435.
22. Edlund, A., Eklöf, S., Sundberg, B., Moritz, T. & Sandberg, G. (1995) *Plant Physiol.* **108**, 1043–1047.
23. Cornish, K. & Zeveaart, J. A. D. (1985) *Plant Physiol.* **76**, 1029–1035.

24. Mitchell, R. E. (1982) *Physiol. Plant Pathol.* **20**, 83–89.
25. Moore, R. A., Starratt, A. N. & Ma, S. W. (1989) *Can. J. Microbiol.* **35**, 910–917.
26. Turlings, T. C. J., Tumlinson, J. H., Heath, R. R., Proveaux, A. T. & Doolittle, R. E. J. (1991) *J. Chem. Ecol.* **17**, 2235–2251.
27. Weber, H., Vick, B. A. & Farmer, E. E. (1997) *Proc. Natl. Acad. Sci. USA* **94**, 10473–10478.
28. Müller, A., Ducting, P. & Weiler, E. W. (2002) *Planta* **216**, 44–56.
29. Engelberth, J., Schmelz, E. A., Alborn, H. T., Cardoza, Y. J., Huang, J. & Tumlinson, J. H. (2003) *Anal. Biochem.* **312**, 242–250.
30. Schmelz, E. A., Alborn, H. T., Banchio, E. & Tumlinson, J. H. (2003) *Planta* **216**, 665–673.
31. Alborn, H. T., Jones, T. H., Stenhagen, G. S. & Tumlinson, J. H. (2000) *J. Chem. Ecol.* **26**, 203–220.
32. Aono, T., Araki, Y., Imanishi, M. & Noguchi, S. (1978) *Chem. Pharm. Bull.* **26**, 1153–1161.
33. Toshima, H. (2001) *J. Synth. Org. Chem.* **59**, 1121–1129.
34. Baldwin, I. T., Zhang, Z. P., Diab, N., Ohnmeiss, T. E., McCloud, E. S., Lynds, G. Y. & Schmelz, E. A. (1997) *Planta* **201**, 397–404.
35. Thomma, B. P., Penninckx, I. A., Broekaert, W. F. & Cammue, B. P. (2001) *Curr. Opin. Immunol.* **13**, 63–68.
36. Bender, C. L., Stone, H. E., Sims, J. J. & Cooksey, D. A. (1987) *Physiol. Mol. Plant Pathol.* **30**, 273–283.
37. Mittal, S. M. & Davis, K. R. (1995) *Mol. Plant–Microbe Interact.* **8**, 165–171.
38. Weiler, E. W., Kutchan, T. M., Gorb, T., Brodschelm, W., Niesel, U. & Bubltz, F. (1994) *FEBS Lett.* **345**, 9–13.
39. Kenyon, J. S. & Turner, J. G. (1992) *Plant Physiol.* **100**, 219–224.
40. Zhao, Y. F., Jones, W. T., Sutherland, P., Palmer, D. A., Mitchell, R. E., Reynolds, P. H. S., Damicone, J. P. & Bender, C. L. (2001) *Physiol. Mol. Plant Pathol.* **58**, 247–258.
41. Volksch, B., Bubltz, F. & Fritsche, W. (1989) *J. Basic Microbiol.* **29**, 463–468.
42. Mitchell, R. E. & Young, H. (1978) *Phytochemistry* **17**, 2028–2029.
43. Kloek, A. P., Verbsky, M. L., Sharma, S. B., Schoelz, J. E., Vogel, J., Klessig, D. F. & Kunkel, B. N. (2001) *Plant J.* **26**, 509–522.
44. Palmer, D. A. & Bender, C. L. (1995) *Mol. Plant–Microbe Interact.* **8**, 683–692.
45. Koda, Y., Takahashi, K., Kikuta, Y., Greulich, F., Toshima, H. & Ichihara, A. (1996) *Phytochemistry* **41**, 93–96.
46. Laudert, D. & Weiler, E. W. (1998) *Plant J.* **15**, 675–684.
47. Hamill, J. D. (1993) *Aust. J. Plant Physiol.* **20**, 405–423.
48. Kettner, J. & Dorffling, K. (1995) *Planta* **196**, 627–634.
49. Stotz, H. U., Koch, T., Biedermann, A., Weniger, K., Boland, W. & Mitchell-Olds, T. (2002) *Planta* **214**, 648–652.
50. Bi, J. L., Murphy, J. B. & Felton, G. W. (1997) *J. Chem. Ecol.* **23**, 1805–1818.
51. Arimura, G., Ozawa, R., Nishioka, T., Boland, W., Koch, T., Kuhnemann, F. & Takabayashi, J. (2002) *Plant J.* **29**, 87–98.
52. Thornburg, R. W. & Li, X. Y. (1991) *Plant Physiol.* **96**, 802–805.
53. Raymond, P., Weber, H., Damond, M. & Farmer, E. E. (2000) *Plant Cell* **12**, 707–719.
54. Frey, M., Stettner, C., Pare, P. W., Schmelz, E. A., Tumlinson, J. H. & Gierl, A. (2000) *Proc. Natl. Acad. Sci. USA* **97**, 14801–14806.
55. Degenhardt, J. & Gershenzon, J. (2000) *Planta* **210**, 815–822.
56. Turlings, T. C. J., Tumlinson, J. H. & Lewis, W. J. (1990) *Science* **250**, 1251–1253.
57. Vet, L. E. M. & Dicke, M. (1992) *Annu. Rev. Entomol.* **37**, 141–172.
58. DeMoraes, C. M., Lewis, W. J., Paré, P. W., Alborn, H. T. & Tumlinson, J. H. (1998) *Nature* **393**, 570–573.
59. Kessler, A. & Baldwin, I. T. (2001) *Science* **292**, 2141–2144.
60. Malamy, J., Carr, J. P., Klessig, D. F. & Raskin, I. (1990) *Science* **250**, 1002–1004.
61. Sanchez-Serrano, J., Amati, S., Ebner, M., Hildmann, T., Mertens, R., Peña-Cortés, H., Prat, S. & Willmitzer, L. (1991) in *Abscisic Acid Physiology and Biochemistry*, eds Davies, H. J. & Jones, H. G. (BIOS Scientific, Lancaster, U.K.), pp. 201–216.
62. Jongsma, M. A., Bakker, P. L., Visser, B. & Stiekema, W. J. (1994) *Planta* **195**, 29–35.
63. Peña-Cortés, H., Sanchez-Serrano, J. J., Mertens, R., Willmitzer, L. & Prat, S. (1989) *Proc. Natl. Acad. Sci. USA* **86**, 9851–9855.
64. Kernan, A. & Thornburg, R. W. (1989) *Plant Physiol.* **91**, 73–78.
65. Birkenmeier, G. F. & Ryan, C. A. (1998) *Plant Physiol.* **117**, 687–693.
66. Zeevaert, J. & Creelman, R. A. (1988) *Annu. Rev. Plant Physiol. Plant Mol. Biol.* **39**, 439–473.
67. Ingram, J. & Bartels, D. (1996) *Annu. Rev. Plant Physiol. Plant Mol. Biol.* **47**, 377–403.
68. Campalans, A., Messegue, R., Goday, A. & Pages, M. (1999) *Plant Physiol. Biochem.* **37**, 327–340.